**Article:**
Bai, L, Fu, J, Pang, L et al. (3 more authors) (2020) Experimental study on a dual compensation chamber loop heat pipe with dual bayonet tubes. Applied Thermal Engineering, 180. 115821. ISSN 1359-4311

https://doi.org/10.1016/j.applthermaleng.2020.115821

# Experimental study on a dual compensation chamber loop heat pipe with dual bayonet tubes

Lizhan Bai Jingwei Fu Liping Pang* Yuandong Guo Guiping Lin

Dongsheng Wen

Laboratory of Fundamental Science on Ergonomics and Environmental Control, School of Aeronautic Science and Engineering, Beihang University, Beijing 100191, PR China

**Abstract:** Dual compensation chamber loop heat pipe (DCCLHP) holds great application potential in the future aircraft thermal management. In this work, a DCCLHP with dual bayonet tubes was proposed and fabricated, aiming to improve its startup performance especially at small heat loads in the terrestrial surroundings. An extensive experimental study was conducted at three typical attitudes of the evaporator/CCs, i.e., the vertical attitude, 45° tilt angle and the horizontal attitude, mainly focusing on its startup characteristics and heat transport capability. According to the experimental results, the DCCLHP with dual bayonet tubes can successfully realize the startup at small heat loads in whatever attitudes of the evaporator/CCs in the ground condition, and reach a heat transport limit greater than 400 W over a distance of 2.0 m. In addition, a new flow mechanism was observed in the experiment, i.e., a local circulation of the working fluid driven by gravity occurred in the loop composed of the evaporator, the CCs, the bayonet tubes, and the branches of the liquid line. This local circulation of working fluid was identified to appear only when the evaporator/CCs were at a certain tilt angle and the heat loads were relatively small.

**Keywords:** loop heat pipe; dual compensation chamber; bayonet tube; startup; heat transport limit



* Corresponding author. Tel.: +86 10 8233 8600; Fax: +86 10 8233 8600

E-mail address: Panglp505@sina.com (L. Pang)

## 1 Introduction

Loop heat pipe (LHP) is a highly efficient and reliable two-phase heat transfer device, which relies on the evaporation and condensation of a working fluid to transfer heat, and the capillary forces developed in the microporous wick to circulate the working fluid where no external power is required [1-3]. Compared with traditional heat pipes, it has the advantage of transporting a larger amount of heat over a longer distance with robust antigravity capability. In addition, its flexible transport lines ensures great adaptability in the installment and arrangement in practical applications [4-8]. At the beginning, LHP was invented for spacecraft thermal control, which has been applied in a wide variety of space missions to address the complex thermal management problems where great success has been achieved [9-14]. With the continuous development and maturity of LHP technology in space thermal control, its application is gradually extending to other areas such as in the aircraft thermal management.

Quite different from the space microgravity environment where LHP with a single compensation chamber (CC) exhibits favorable operation performance, in the aircraft thermal management gravity and acceleration play an important role in the LHP operation especially when the attitude of the aircraft keeps varying. That is because in the terrestrial surroundings, once the CC is located below the evaporator, liquid working fluid will accumulate in the CC due to the gravity effect. It will cause a difficulty in the liquid supply to the evaporator wick, and under which condition the normal operation of the LHP will be disrupted, leading to an operating failure of the LHP [15-18]. Although sometimes the employment of a secondary wick hydrodynamically connecting the primary wick and the CC can help guarantee the liquid supply to the evaporator in an adverse attitude, because the liquid flow resistance in the secondary wick is relatively large, it will inevitably result in a considerable reduction in the heat transport capability.

To solve this issue mentioned above, dual compensation chamber loop heat pipe (DCCLHP) was proposed,

where two CCs were employed located at each end of the evaporator [19, 20]. Thanks to this novel design, the DCCLHP is able to achieve sufficient liquid supply to the evaporator wick at whatever orientations, and it is expected to function in any orientation in the terrestrial surroundings. As a result, the DCCLHP shows great application potential in the aircraft thermal management system.

So far, the DCCLHP has been experimentally studied by a few researchers, as briefly reviewed below. Gluck et al. [20] carried out the performance tests of a DCCLHP at the Air Force Research Laboratory (AFRL), and compared the experimental results with those obtained at the Institute of Thermal Physics (ITP) in Russia. It was found that at the steady state, the operating temperatures were higher and heat transfer coefficients and thermal conductance were lower at AFRL. The authors ascribed these differences to higher resistance due to usage, rather than test, mounting and more complex insulation lay-up at AFRL. AFRL transient data also showed brief reverse flow on startup for some runs with power at or below 50 W, and at times marked temperature fluctuations. Bai et al. [21] investigated the startup characteristics of a DCCLHP with a small heat load of 5 W applied to the evaporator. The prototype exhibited four situations in the startup process under three different attitudes. In most of the experiments, the DCCLHP could start up reliably; however, rather large temperature overshoot occurred sometimes. The main reason lay in the heat leak from the evaporator to the CC, resulting in a small temperature difference between them, and under which condition the saturation pressure difference between the evaporator and the CC was not sufficient to drive the positive flow of the working fluid in the loop. Lin et al. [22] developed a DCCLHP to solve the problem of relative orientation limit between the evaporator and the CC, and presented the design method of working fluid inventory together with the CC volume. Test results validated the design method, and the startup characters were tested in three different orientations. Lin et al. [23] conducted a partial visualization study of a DCCLHP with both CCs and the condenser covered by transparent crystal glass. The DCCLHP could operate steadily with the heat load

over 50 W, and a typical V-shaped curve of operation temperature was obtained. However, some unstable phenomena during the startup were revealed, which appeared with the application of heat load. Feng et al. [24] investigated the operating instability of a DCCLHP including temperature hysteresis, reverse flow and temperature oscillation, and explained the reverse flow during the startup. Nine conditions concerning the gravity effect and evaporator/CC orientation were taken into account. Therefore, the startup of a DCCLHP also requires a suitable liquid/vapor distribution and temperature difference between the evaporator and CC, which is coincident to that of the conventional LHP with a single CC. Due to the operation suitability of DCCLHP in the acceleration field, Xie et al. [25, 26] studied the transient characteristics of a DCCLHP under different acceleration forces up to 11g in different directions. The DCCLHP failed to start up at a heat load of 80 W in the terrestrial surroundings. It could start up at a heat load greater than 100 W, but with different startup behaviors under different acceleration direction and magnitude. In some particular acceleration directions, the centrifugal force could assist DCCLHP to start up successfully and obtain a lower operating temperature due to the easier liquid return, which could produce a relatively large temperature difference between the evaporator and CCs.

By analyzing the previous experimental results above, it can be concluded that the DCCLHP can indeed realize an orientation-free operation in the terrestrial or acceleration surroundings, exhibiting great application potential in the aircraft thermal management. However, generally a steady operation of the DCCLHP can only be achieved at a heat load greater than 100 W. If the heat load applied to the evaporator is relatively small, i.e., 50 W or even lower, a startup failure may occur, accompanied by some operating instability phenomena such as reverse flow, strong temperature oscillation and large temperature overshoot, which greatly obstructs the future practical applications of the DCCLHP.

Through a careful analysis of the energy balance in the evaporator and the CCs, the significantly degraded

thermal performance of the DCCLHP at small heat loads should be closely associated with its particular structure. In a conventional DCCLHP, a bayonet tube is usually employed travelling through one CC and extending to the middle point of the evaporator core. For this particular design, the CC with the bayonet tube travelling through (represented by CC1) can always receive good cooling from the return subcooled liquid in any orientation in the terrestrial surroundings. As the return liquid flows towards the CC without the bayonet tube travelling through (represented by CC2), it is heated by the heat leak from the evaporator whose temperature increases gradually. Especially when the heat load is small, the mass flowrate of the working fluid in the loop is very small accordingly, and the return liquid will have a rather small subcooled degree when it is approaching the CC2. As a result, the CC2 obviously receives much worse cooling effect from the return liquid than the CC1. When the CC2 is located above the evaporator, the vapor bubbles generated in the evaporator core will flow into the CC2 due to the buoyancy effect as evidenced by our previous visualization study [23], causing a large amount of heat leak from the evaporator to the CC2. Under this condition, significant energy imbalance for the CC2 due to large heat leak and weak cooling should be responsible for the startup failure and the associated operating instability phenomena.

In order to solve this issue mentioned above, an improved DCCLHP, i.e., a DCCLHP with dual bayonet tubes, is proposed and fabricated in this work. For this innovative DCCLHP, two bayonet tubes are employed, travelling through the CCs at each end of the evaporator respectively. By means of this novel design, the return subcooled liquid is divided into two parts before entering the CCs, and each part is then routed to flow through each CC respectively. Under this condtion, each CC can receive good cooling from the return liquid in any orientation in the terrestrial surroundings, and good startup performance and stable operation can be expected. An extensive experimental study on this innovative DCCLHP is carried out, mainly focusing on its startup characteristics and heat transport capability, and some important conclusions have been reached, as reported

and analyzed below.

## 2 Experimental system

Fig. 1 shows a schematic view of the experimental system in this work, which consists of a DCCLHP with dual bayonet tubes, heat source, heat sink, and the temperature measurement and data acquisition system. Fig.2 shows the structure of the evaporator/CCs with dual bayonet tubes. Ammonia was selected as the working fluid for its relatively large Durbar parameter. Moreover, the value d$P$/d$T$ of the working fluid should also be sufficiently large to ensure a successful startup at a minimum temperature difference between the evaporator and the CCs. According to this criterion, ammonia is considered the best working fluid in the operating temperature range of -60 ~ +60 ℃.

The DCCLHP investigated in this work was composed of an evaporator (EVA), a condenser (CON), CC1, CC2, vapor line, liquid line, and dual bayonet tubes. Different from a traditional DCCLHP with only a single bayonet tube extending into the middle point of the evaporator core, dual bayonet tubes were adopted here travelling through two CCs respectively. The two CCs were of the same size, integrated with the evaporator coaxially. Moreover, a serpentine condenser was soldered to one side of an aluminum plate with fins at the other side to increase the heat transfer area. The aluminum plate was cooled by air natural or forced convention for heat dissipation to the environment. The DCCLHP was made of stainless steel except that the evaporator wick was made of nickel powders. Table  presents the basic parameters of the tested DCCLHP.

A thin film electric resistance heater was attached tightly on the evaporator casing to simulate the heat source. The heater was connected to a DC power supply directly, which could be adjusted continuously from 0 to 500 W by altering the output voltage. The maximum uncertainty of the heat load was within ±5.0 %. In the experiment, the tested DCCLHP was placed on a horizontal plane, ignoring the anti-gravity effects. Type T thermocouples with the maximum measurement uncertainty of about ± 0.5℃ were adopted to monitor the

temperature profile along the loop. Eight thermocouples were attached on some key points along the loop, as illustrated in Fig. 3. Meanwhile, the room temperature was also measured and recorded. In order to simulate the real situation of DCCLHP application as much as possible, no thermal insulation was adopted for the casing of the DCCLHP in the experiment. Only the thermocouple junction was covered by a layer of thermal insulation material to reduce the heat transfer to the ambient surroundings, so that the measured wall temperatures should be very close to the temperatures of the working fluid inside, as the wall thickness was no more than 1.0 mm for all the LHP components. Three typical attitudes of the evaporator/CCs of the DCCLHP, i.e., the vertical attitude, 45° tilt angle and the horizontal attitude, were tested, as shown in Fig. 4.

## 3 Experimental results and discussions

### 3.1 Startup characteristics

For a LHP-based thermal management system, successful startup is always the prerequisite to realize the practical applications. Typically, a LHP can realize self-startup without any preconditioning. However, self-startup does not mean instant startup, and the startup may take a long time accompanied by very large evaporator temperature rise even exceeding the maximum allowable temperature. As a two-phase heat transfer device, the startup of a LHP is a very complex dynamic process, ranging from the application of a heat load to the evaporator to the normal circulation of working fluid in the loop. During this process, a variety of heat transfer phenomena in quite different forms may be involved such as evaporation, boiling, condensation, conduction and convection, accompanied by complicated liquid/vapor movement and phase redistribution. According to previous studies, the startup of a LHP is affected by multiple factors such as the initial liquid/vapor distribution in the evaporator and the heat load applied to the evaporator. Based on the initial liquid/vapor distribution in the evaporator, four possible startup situations have been identified, as listed in Table 2 [2]. Many experiments have shown that LHPs are the easiest to start up in situation 2, but the most

difficult in situation 3.

### 3.1.1 Vertical attitude

Figs. (5-8) show the temperature changes of some key points along the loop during the startup when the evaporator/CCs of the DCCLHP is in the vertical attitude, where the startup heat loads are 5, 10, 40 and 80 W respectively. In the experiments, the evaporator was always kept horizontal with the condenser, i.e., no adverse elevation existed. The room temperature was maintained at about 20 °C. As the evaporator heat load was relatively small, i.e., < 100 W, the fan was not switched on, and the heat transfer from the aluminum plate with fins to the environment was totally in the form of air natural convection.

As shown in Fig. 5, when a heat load of 5 W was applied to the evaporator, the evaporator temperature rose immediately followed by the evaporator outlet temperature, suggesting an instant occurrence of evaporation in the vapor grooves. Under this condition, vapor should exist in the vapor grooves. Otherwise if the vapor grooves are flooded by liquid, an obvious superheat will be required to initiate the nucleate boiling there. At the same time, the CC2 temperature also rose quickly, which was always keeping close to the evaporator outlet temperature. That is because the heat leak from the evaporator to the CC2 is very large. It can be inferred that vapor or gas bubbles should exist in the evaporator core, and the heat leak from the evaporator to the CC2 is in the form of evaporation and condensation, just like the phenomena occurring in a conventional heat pipe. Based on the analysis above, this startup is corresponding to the situation 4 in Table 2.

With the circulation of the working fluid in the loop, the vapor generated in the evaporator entered the condenser, and the condenser inlet temperature rose sharply, approaching the evaporator outlet temperature. Once vapor entered the condenser, the heat load applied to the evaporator can be efficiently dissipated to the ambient, and under this condition the evaporator temperature began to tend to stability after a slight drop, producing a small peak. The temperature at the middle point of the condenser was obviously lower than the

evaporator outlet temperature, indicating that vapor did not reach there, and the utilization efficiency of the condenser was less than one half. Although the utilization efficiency of the condenser was relatively low, because the heat load applied to the evaporator was very small, i.e., only 5 W, the evaporator could also reach a very low steady state operating temperature.

As shown in Fig. 6, when a heat load of 10 W was applied to the evaporator, the variations of the key points along the loop were very similar to those in Fig. 5, i.e., the startup also proceeded in situation 4, and a small peak appeared for the evaporator temperature. Through a careful analysis, there existed obviously two differences. First, when the heat load was increased from 5 to 10 W, the startup time became much shorter. For instance, at a heat load of 5 W, it took about 8 mins for the evaporator temperature to reach its peak value; however, this time was reduced to about 3 mins at a heat load of 10 W. Second, when the heat load was increased from 5 to10 W, the utilization efficiency of the condenser obviously became larger. For instance, at a heat load of 5 W, the utilization efficiency of the condenser was less than one half; however, it was increased to greater than one half at a heat load of 10 W, as evidenced by the fact that the temperature at the middle point of the condenser was very close to the evaporator outlet temperature after the startup. Because of the notably increased utilization efficiency of the condenser, the steady state operating temperature at a heat load of 10 W was very close to that at a heat load of 5 W, and they were both slightly lower than 25 °C.

As shown in Figs. 7 and 8, when the heat loads applied to the evaporator were further increased to 40 and 80 W, the temperature variations of the key points along the loop of the DCCLHP were quite similar to those when the heat loads were 5 and 10 W. The main difference was that the steady state operating temperature of the DCCLHP was significantly increased due to the increase of the heat load. It should be of note that when the evaporator/CCs were in the vertical attitude, the heat leak from the evaporator would be mainly transferred to the CC at the top (CC2 in Fig. 4), because the vapor bubbles generated in the evaporator core flowed

upwards into the CC due to the effect of buoyancy in the terrestrial surroundings, and the heat leak from the evaporator to the CC at the bottom (CC1 in Fig. 4) was very small accordingly. As a result, the temperature difference between the CC2 and CC1 was rather large during the startup process. For instance, in Fig. 7, the CC2 temperature increased to about 65 °C at 100 minutes, while the CC1 temperature almost always remained at about 19 °C, causing a quite large temperature difference up to 46 °C.

For the DCCLHP with dual bayonet tubes, when the evaporator/CCs were at the vertical attitude, a unique phenomenon was observed during the startup, i.e., the temperature at the CC2 inlet was very close to the saturation temperature of the working fluid. Generally, for a conventional LHP with a single CC or a conventional DCCLHP with a single bayonet tube, the temperature at the CC inlet should be obviously lower than the saturation temperature during the startup to provide efficient cooling to the CC, which is essential for the normal operation of the LHP. Once the temperature at the CC inlet increases to approach the saturation temperature, a reverse flow of the working fluid should occur followed by the resultant startup failure. For DCCLHP with dual bayonet tubes, the situation becomes much different, and a new flow mechanism appears depending on the competition between natural circulation driven by temperature difference and forced flow driven by capillary pressure. As shown in Fig. 9 (a), the evaporator, the CCs, the bayonet tubes, and the branches of the liquid line together construct a loop. As the working fluid in the evaporator core has a higher temperature, while the working fluid in the branches of the liquid line has a lower temperature, this temperature difference will lead to an obvious density difference, which can induce a natural circulation of the working fluid in the loop due to the pressure imbalance, i.e., the working fluid in the evaporator core flows upwards exiting the CC2, and the working fluid in the branches of the liquid line flows downwards, which mixes with the return subcooled liquid at the junction and then enters the CC1, forming a local circulation. It should be of note that this local natural circulation of the working fluid driven by the temperature difference only occurs

when the heat load applied to the evaporator is relatively small, i.e., < 100 W. At a large heat load, as the mass flowrate of the working fluid increases to a relatively large value, the forced flow driven by the capillary pressure in the liquid line will overwhelm this natural circulation, and as a result, the return subcooled liquid flows into each CC through the dual bayonet tubes respectively, as shown in Fig. 9 (b).

**3.1.2 45° tilt angle**

Figs. 10 and 11 show the temperature changes of some key points along the loop during the startup when the evaporator/CCs of the DCCLHP is at the 45° tilt angle, where the startup heat loads are 40 and 60 W respectively. In the experiments, the operating conditions for the DCCLHP were all the same as those in Figs. (5-8), i.e., the evaporator was always kept horizontal with the condenser, and the heat transfer from the aluminum plate with fins to the environment was in the form of air natural convection.

As shown in Figs. 10 and 11, when the evaporator/CCs of the DCCLHP was at the 45° tilt angle, the temperature changes of the key points along the loop during the startup were quite similar to those in Figs. 7 and 8. In Figs. 10 and 11, during the startup, the CC1 temperature was the lowest and remained almost unchanged, indicating that the heat leak from the evaporator to the CC1 was rather small, which can be generally neglected. While the CC2 temperature was very close to the evaporator temperature, which showed that the heat leak from the evaporator to the CC2 was very large. At the same time, the temperature at the CC2 inlet was much higher than that at the CC1 inlet, which coincided with the cases in Figs. 7 and 8. Finally, the DCCLHP reached a steady state and finished the startup.

**3.1.3 Horizontal attitude**

Figs. 12 and 13 show the temperature changes of some key points along the loop during the startup when the evaporator/CCs of the DCCLHP is at the horizontal attitude, where the startup heat loads are 40 and 60 W respectively. In the experiments, the operating conditions for the DCCLHP were all the same as those in Figs.

(5-8), i.e., the evaporator was always kept horizontal with the condenser, and the heat transfer from the aluminum plate with fins to the environment was in the form of air natural convection.

As shown in Fig. 12, when a heat load of 40 W was applied to the evaporator, the evaporator temperature rose immediately followed by the evaporator outlet temperature, indicating that liquid evaporation occurred in the vapor grooves instantly, and the generated vapor flowed out of the evaporator. It can be inferred that vapor should exist in the vapor grooves initially. At the same time, both CC1 and CC2 temperature rose quickly with the evaporator temperature. That is because the heat leak from the evaporator to the CC1 and CC2 is very large. This phenomenon was obviously different from the cases when the evaporator/CCs were at the vertical attitude or 45° tilt angle, under which condition only the temperature of the CC located above rose quickly, while the other CC temperature remained almost unchanged. Another obvious difference was that in Fig. 12, the temperature at the CC2 inlet always remained almost unchanged; while when the evaporator/CCs were at the vertical attitude or 45° tilt angle, the temperature at the CC2 inlet rose quickly approaching approximately the evaporator temperature. It indicated that when the evaporator/CCs were at the horizontal attitude, because of the absence of the gravity effect, the local natural circulation would no longer occur, and the returning subcooled liquid driven by the capillary pressure almost evenly entered the two CCs, as shown in Fig. 9 (b). From the quickly increasing CC1 and CC2 temperature, it can be inferred that vapor or gas bubbles should exist in the evaporator core, and the heat leak from the evaporator to the CC1 and CC2 was in the form of evaporation and condensation, just like the phenomena happening in a conventional heat pipe. Based on the analysis above, this startup is also corresponding to the situation 4 in Table 2.

During the startup process, it should be of note that the CC1 temperature always kept higher than the CC2 temperature, indicating that the heat leak from the evaporator to the CC1 and CC2 was not equal, and the heat leak to the CC1 should be larger than that to the CC2. With the circulation of the working fluid in the loop, the

vapor generated in the evaporator entered the condenser, and the condenser inlet temperature rose quickly, approaching the evaporator outlet temperature. The temperature at the middle point of the condenser was obviously lower than the evaporator outlet temperature, indicating that vapor did not reach there, and the utilization efficiency of the condenser was less than one half. At about 45 min, the evaporator temperature began to rise very slowly, and gradually approach a steady state.

As shown in Fig. 13, at a heat load of 60 W, the temperature changes of the characteristic points along the loop were quite similar to those in Fig. 12. Comparing Fig. 13 with Fig. 12, it is easy to find that the steady state operating temperature at a heat load of 60 W is lower than that at a heat load of 40 W, which well reflects the character of variable conductance of the LHP. That is because the utilization efficiency of the condenser increases with the increase of the heat load, as evidenced by the increase of the temperature at the middle point of the condenser, resulting in the decrease of the operating temperature of the LHP.

**3.1.4 Effect of antigravity on the startup**

It is well known that the strong capability of antigravity operation is an obvious advantage for LHPs compared with conventional heat pipes. Figs. 14 and 15 show the temperature changes of some characteristic points along the loop during the startup with a heat load of 20 W and 30 W respectively, when the evaporator/CCs were in the vertical attitude and the evaporator was horizontal with the condenser, i.e., no adverse elevation existed. As a comparative study, Figs. 16 and 17 show the startup processes of the DCCLHP at a heat load of 20 W and 30 W respectively, when the evaporator/CCs were in the vertical attitude and the evaporator was located 0.3 m higher than the condenser, i.e., the adverse elevation was 0.3m.

Comparing Fig. 16 with Fig. 14, the DCCLHP can successfully realize the startup at a startup heat load of 20 W when the evaporator is horizontal with or higher than the condenser. However, the existence of adverse elevation results in an increase of the steady state operating temperature. When the evaporator is horizontal

with the condenser, the steady state operating temperature of the DCCLHP is about 50.2 °C; while when the evaporator is 0.3m higher than the condenser, the steady state operating temperature is increased to about 52.1 °C. Comparing Fig. 17 with Fig. 15, the DCCLHP can successfully realize the startup at a startup heat load of 30 W when the evaporator is horizontal with or higher than the condenser. However, the existence of adverse elevation results in an increase of the steady state operating temperature. When the evaporator is horizontal with the condenser, the steady state operating temperature of the DCCLHP is about 62.3 °C; while when the evaporator is 0.3m higher than the condenser, the steady state operating temperature is increased to about 65.2 °C.

The existence of adverse elevation will cause an additional pressure drop in the external loop, resulting in increased saturation temperature difference between the evaporator and the CC, and the resultant increased heat leak from the evaporator to the CC will inevitably lead to an increase of the operating temperature. As shown in Figs. 16 and 17, due to the increase in the operating temperature, the vapor generated in the evaporator fully condenses into liquid before it enters the condenser, as evidenced by the sudden drop of the temperature at the inlet of the condenser. Under this condition, the condenser is in fact not effectively used, which can explain the very high operating temperature from another aspect.

**3.2 Heat transfer capability**

The heat transfer capability characterizes the maximum heat load that the DCCLHP evaporator can sustain over a fixed heat transport distance. Once the heat load applied to the evaporator exceeds its maximum allowable value, the DCCLHP evaporator temperature would continue to rise causing serious accidents such as the burnout of the device to be cooled, which should be strictly prohibited in the practical applications. For LHPs, the heat transfer capability is mainly determined by the capillary limit. It means that at this maximum heat load, the total pressure drop of the working fluid in the loop is just equal to the maximum capillary

pressure developed in the evaporator wick. Beyond this value, the capillary pressure will be insufficient to drive the normal circulation of the working fluid, leading to the resultant operation failure.

### 3.2.1 Vertical attitude

Fig. 18 shows the experimental results of the power increment test of the DCCLHP when the evaporator/CCs is at the vertical attitude. In the experiment, the fan was always kept in operation, so that the finned aluminum plate was cooled by air forced convection. The middle point of the evaporator and the condenser was in a horizontal plane, i.e., no adverse elevation existed. The heat load was increased stepwisely following 100W-200W-300W-350W-370W-380W-390W-400W, and the evaporator temperature change was monitored carefully as well as the temperatures at some key points along the loop. At each heat load, it should allow the DCCLHP to reach the steady state operation. As shown in Fig. 18, when the heat load was increased from 100W to 200W, the operating temperature dropped obviously, indicating that the DCCLHP was operating in the variable conductance mode, and the utilization efficiency of the condenser increased with the increase of the heat load. At the same time, the temperature at the CC2 inlet also dropped sharply from 44.2 °C to 23.4 °C, which should correspond to the transition of the flow mechanism from local natural circulation to forced flow, due to an enhancement of the forced flow driven by the capillary pressure, as analyzed previously in the last part in section 3.1.1.

Starting from the heat load of 200W, the operating temperature began to increase with increasing heat load, indicating that the DCCLHP was operating in the constant conductance mode. It was found that starting from 350W, the temperature at the condenser middle point showed a slowly decreasing trend. It can be inferred that a recession for the liquid/vapor interface should occur in the condenser. When the heat load was 390W, the evaporator could operate stably around 53 °C. However, when the heat load was further increased to 400W, the evaporator temperature began to rise continuously up to 70 °C with no trend to reach a steady state,

indicating that the DCCLHP reached its heat transfer limit.

### 3.2.2 45° tilt angle

Fig. 19 shows the experimental results of the power increment test of the DCCLHP when the evaporator/CCs is at the 45° tilt angle. The other operating conditions were all the same as those in Fig. 18. In Fig. 19, the heat load was increased stepwisely following 100W-200W-300W-350W-370W-390W-410W-430W-450W. Similar to the case in Fig.18, in Fig.19 when the heat load was increased from 100W to 200W, the operating temperature dropped obviously, indicating that the DCCLHP was operating in the variable conductance mode. At the same time, the temperature at the CC2 inlet also dropped sharply from 35.3 °C to 22.4 °C, which should correspond to the transition of the flow mechanism from local natural circulation to forced flow.

Starting from the heat load of 200W, the operating temperature began to increase with increasing heat load, indicating that the DCCLHP was operating in the constant conductance mode. It was found that starting from 370W, the temperature at the condenser middle point showed a slowly decreasing trend. It can be inferred that a recession for the liquid/vapor interface should occur in the condenser. When the heat load was 430W, the evaporator could operate stably around 51 °C. However, when the heat load was further increased to 450W, the evaporator temperature began to rise continuously with no trend to reach a steady state, indicating that the DCCLHP reached its heat transfer limit.

### 3.2.3 Horizontal attitude

Fig. 20 shows the experimental results of the power increment test of the DCCLHP when the evaporator/CCs is at the horizontal attitude with an adverse elevation of 0.1 m. The other operating conditions were all the same as those in Fig. 18. In Fig. 20, the heat load was increased stepwisely following 100W-200W-300W-350W-370W. When the heat load was increased from 100W to 200W, the operating temperature dropped slightly, i.e., only about 3.2 °C, indicating that the DCCLHP was operating in the variable conductance mode.

Different from the cases in Figs. 18 and 19, in Fig. 20 the temperature at the CC2 inlet always remained almost unchanged at the ambient temperature, due to the absence of the gravity effect in the horizontal attitude, and under which condition the local natural circulation of the working fluid could never occur.

Starting from the heat load of 200W, the operating temperature began to increase with increasing heat load, indicating that the DCCLHP was operating in the constant conductance mode. It was found that starting from 300W, the temperature at the condenser middle point showed a slowly decreasing trend. It can be inferred that a recession for the liquid/vapor interface should occur in the condenser. When the heat load was 350W, the evaporator could operate stably around 48.7 °C. However, when the heat load was further increased to 370W, the evaporator temperature began to rise continuously with no trend to reach a steady state, indicating that the DCCLHP reached its heat transfer limit. Compared with the experimental results in Figs. 18 and 19, the heat transport capability of the DCCLHP is obviously reduced due to the existence of an adverse elevation, which produces an additional pressure drop for the liquid flow in the liquid line.

## 4 Conclusions

In order to solve the startup difficulty for the DCCLHP especially at a small heat load in an unfavorable attitude, an innovative DCCLHP with dual bayonet tubes was proposed and developed in this work. Extensive experimental studies have been conducted on this new type DCCLHP mainly focusing on the startup and heat transport capability at three typical attitudes of the evaporator/CCs. Some interesting phenomena were observed and theoretically analyzed. Based on the experimental results, some important conclusions have been drawn, as summarized below:

- This work validated experimentally that the DCCLHP with dual bayonet tubes could overcome the limitation of the relative orientation between the evaporator and the CCs and successfully realize the startup even at a very small heat load in the terrestrial surroundings, exhibiting great application

potential in the future aircraft thermal management.

- The DCCLHP showed good anti-gravity performance. It could realize the startup with an adverse elevation of 0.3 m. However, the presence of anti-gravity would result in the increase of the steady-state operating temperature.
- A new flow mechanism was observed in the experiment: when the evaporator/CCs was at a tilt angle, a local natural circulation of the working fluid occurred in the evaporator at small heat loads, causing obviously different temperature distribution along the loop. When the evaporator/CCs was at the horizontal attitude, this local natural circulation could no longer happen.
- The DCCLHP could achieve a heat transfer capacity of about 430 W over a transport distance of 2.0 m.

## Acknowledgement

This work was supported by the Beijing Natural Science Foundation (No. 3182023), and the National Natural Science Foundation of China (Nos. 51576010 and 51776012).

## References

[1] Y.F. Maydanik, Loop heat pipes, Applied Thermal Engineering, 25(5-6) (2005) 635-657.

[2] J. Ku, Operating characteristics of loop heat pipes, SAE Paper, No. 0148-7191,1999.

[3] Y.F. Maydanik, M.A. Chernysheva, V.G. Pastukhov, Review: Loop heat pipes with flat evaporators, Applied Thermal Engineering, 67(1-2) (2014) 294-307.

[4] A. Ambirajan, A.A. Adoni, J.S. Vaidya, et al, Loop Heat Pipes: A Review of Fundamentals, Operation and Design, Heat Transfer Engineering, 33(4-5) (2012) 387-405.

[5] K. Nakamura, K. Odagiri, H. Nagano, Study on a loop heat pipe for a long-distance heat transport under anti-gravity condition, Applied Thermal Engineering, 107 (2016) 167-174.

[6] M.A. Chernysheva, Y.F. Maydanik, J.M. Ochterbeck, Heat transfer investigation in evaporator of loop heat pipe during startup, Journal of Thermophysics and Heat Transfer, 22 (2008) 617-622.

[7] K. Odagiri, H. Nagano, Investigation on liquid-vapor interface behavior in capillary evaporator for high heat flux loop heat pipe, International Journal of Thermal Sciences, 140 (2019) 530-538.

[8] V.S. Jasvanth, Abhijit A. Adoni, V. Jaikumar, et al., Design and testing of an ammonia loop heat pipe, Applied Thermal Engineering 111 (2017) 1655-1663.

[9] Y. Maydanik, V. Pastukhov, M. Chernysheva, Development and investigation of a loop heat pipe with a high heat-transfer capacity, Applied Thermal Engineering 130 (2018) 1052-1061.

[10] Y. Guo, G. Lin, J. He, et al, Experimental study on the supercritical startup and heat transport capability of a neon-charged cryogenic loop heat pipe, Energy Conversion and Management, 134 (2017) 178-187.

[11] J. He, J. Miao, L. Bai, et al., Effect of non-condensable gas on the startup of a loop heat pipe, Applied Thermal Engineering 111 (2017) 1507-1516.

[12] T. Tharayil, L.G. Asirvatham, S. Rajesh, et al., Thermal Management of Electronic Devices Using

Combined Effects of Nanoparticle Coating and Graphene-Water Nanofluid in a Miniature Loop Heat Pipe, IEEE Transactions on Components, Packaging and Manufacturing Technology 8 (2018) 1241-1253.

[13] Y. Guo, G. Lin, J. He, et al, Experimental analysis of operation failure for a neon cryogenic loop heat pipe, International Journal of Heat and Mass Transfer, 138 (2019) 96-108.

[14] M. Nishikawara, H. Nagano, Parametric experiments on a miniature loop heat pipe with PTFE wicks, International Journal of Thermal Sciences, 85 (2014) 29-39.

[15] N.S. Ramasamy, P. Kumar, B. Wangaskar, et al., Miniature ammonia loop heat pipe for terrestrial applications: Experiments and modeling, International Journal of Thermal Sciences 124 (2018) 263-278.

[16] G. Zhou, J. Li, L. Lv, An ultra-thin miniature loop heat pipe cooler for mobile electronics, Applied Thermal Engineering, 109 (2016) 514-523.

[17] L. Bai, J. Fu, G. Lin, et al., Quiet power-free cooling system enabled by loop heat pipe, Applied Thermal Engineering 155 (2019) 14-23.

[18] J. Li, L. Lv, Performance investigation of a compact loop heat pipe with parallel condensers, Experimental Thermal and Fluid Science, 62 (2015) 40-51.

[19] C. Gerhart, D. Gluck, Summary of operating characteristics of a dual compensation chamber loop heat pipe in gravity, 11th International Heat Pipe Conference, Tokyo, Japan, 1999.

[20] D. Gluck, C. Gerhart, S. Stanley, Characterization of a high capacity, dual compensation chamber loop heat pipe, AIP Conference Proceedings, 1999, pp. 943-948.

[21] L. Bai, G. Lin, D. Wen, et al., Experimental investigation of startup behaviors of a dual compensation chamber loop heat pipe with insufficient fluid inventory, Applied Thermal Engineering, 29 (2009) 1447-1456.

[22] G. Lin, H. Zhang, X. Shao, et al., Development and test results of a dual compensation chamber loop heat pipe, Journal of Thermophysics and Heat Transfer, 20 (2006) 825-834.

[23] G. Lin, N. Li, L. Bai, et al., Experimental investigation of a dual compensation chamber loop heat pipe, International Journal of Heat and Mass Transfer, 53 (2010) 3231-3240.

[24] J. Feng, G. Lin, L. Bai, Experimental investigation on operating instability of a dual compensation chamber loop heat pipe, Science in China Series E: Technological Sciences, 52 (2009) 2316-2322.

[25] Y. Xie, Y. Zhou, D. Wen, et al, Experimental investigation on transient characteristics of a dual compensation chamber loop heat pipe subjected to acceleration forces, Applied Thermal Engineering, 130 (2018) 169-184.

[26] Y. Xie, J. Zhang, L. Xie, et al, Experimental investigation on the operating characteristics of a dual compensation chamber loop heat pipe subjected to acceleration field, Applied Thermal Engineering, 81 (2015) 297-312.

## Table captions

Table 1 Basic parameters of the tested DCCLHP

Table 2 Liquid/vapor distribution in the evaporator

## Figure captions

Table 1 Basic parameters of the tested DCCLHP

| Components | Parameter | Dimensions | Material |
|---|---|---|---|
| Evaporator | Casing OD/ID ×length/mm | 18/16×150 | Stainless steel |
| | Wick OD/ID ×length/mm | 16/6×120 | Nickel |
| Vapor line | OD/ID ×length/mm | 3/2×1800 | Stainless steel |
| Condenser line | OD/ID ×length/mm | 3/2×2400 | Stainless steel |
| Liquid line | Vapor line OD/ID ×length/mm | 3/2×1800 | Stainless steel |
| Wick | Porosity | 55.0% | —— |
| | Maximum capillary radius/μm | 1.0 | —— |
| CC | Volume/ml | 24.7 | Stainless steel |

Table 2 Liquid/vapor distribution in the evaporator

| Situations | Vapor grooves/evaporator core |
|---|---|
| 1 | Liquid filled/liquid filled |
| 2 | Vapor exists/ liquid filled |
| 3 | Liquid filled /vapor exists |
| 4 | Vapor exists/vapor exists |

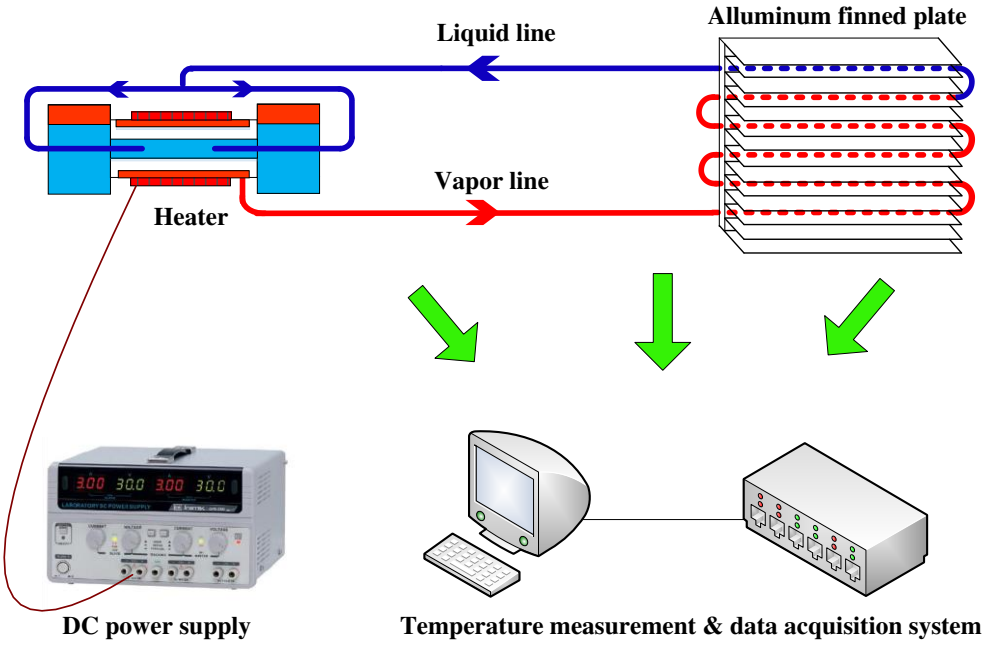


Fig. 1 Schematic of the experimental system of the DCCLHP

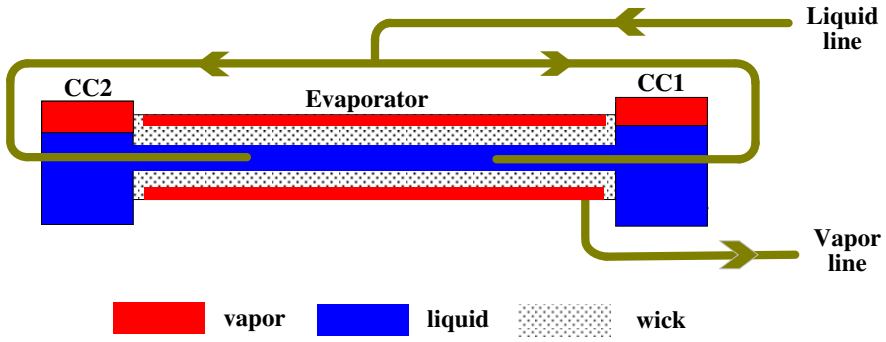


a) Schematic view of the evaporator/CCs

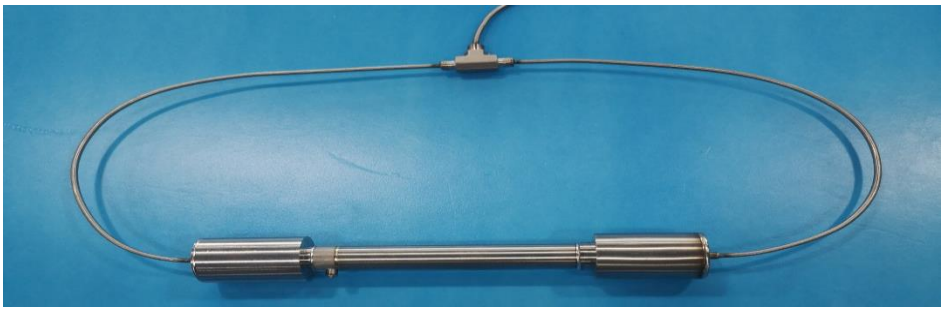

b) Photo of the evaporator/CCs

Fig. 2 Evaporator/CCs with dual bayonet tubes

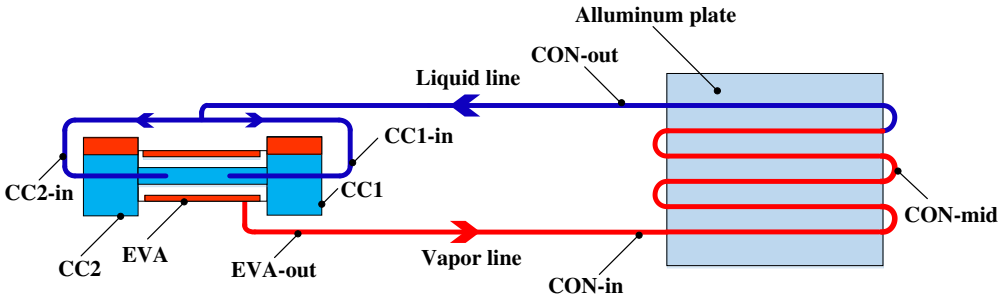


Fig. 3 Thermocouple locations along the DCCLHP in the experiment

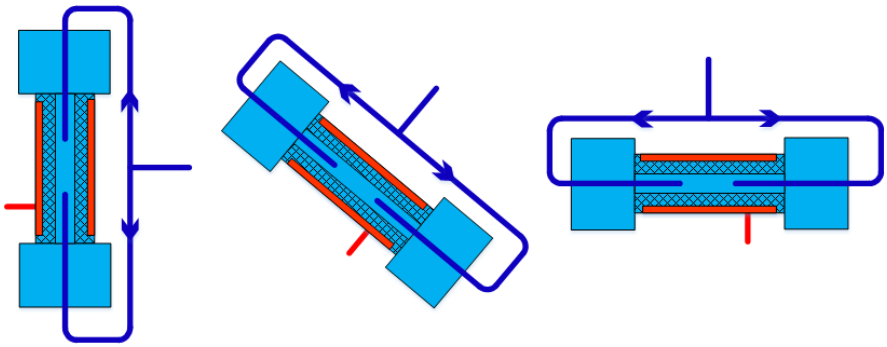

(a) vertical attitude (b) 45° tilt angle (c) horizontal attitude

Fig. 4 Three typical attitudes of the evaporator/CCs in the experiment

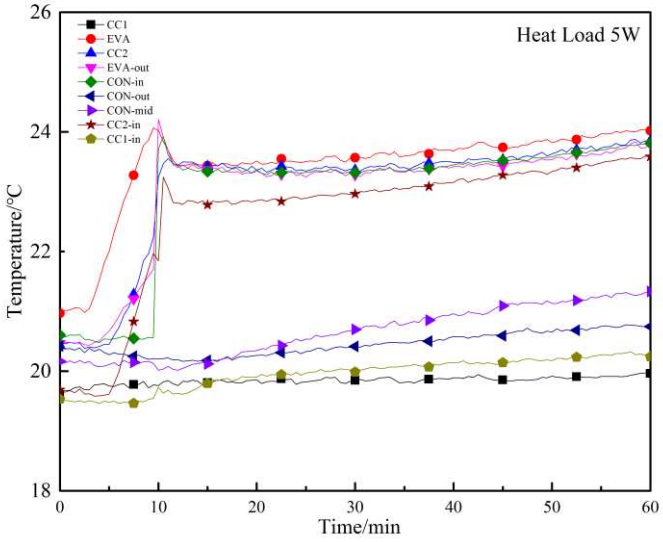


Fig. 5 Startup at a heat load of 5W in the vertical attitude

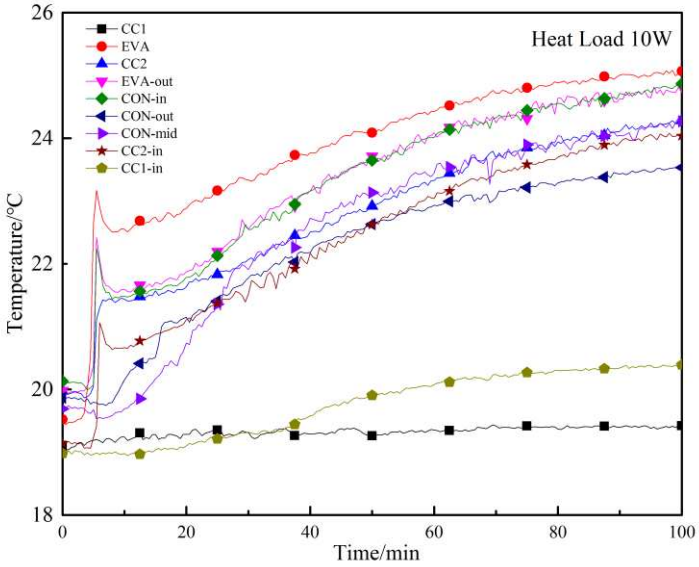


Fig. 6 Startup at a heat load of 10W in the vertical attitude

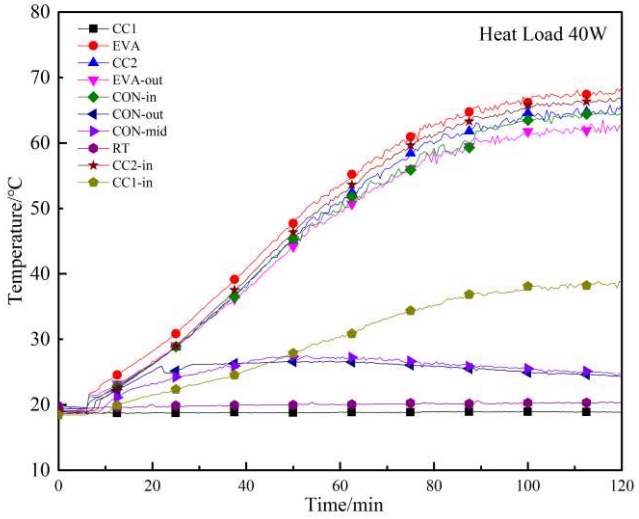


Fig. 7 Startup at a heat load of 40W in the vertical attitude

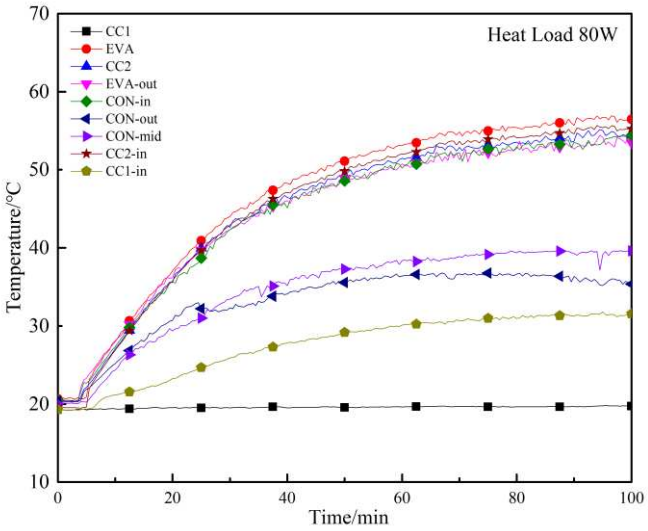


Fig. 8 Startup at a heat load of 80W in the vertical attitude

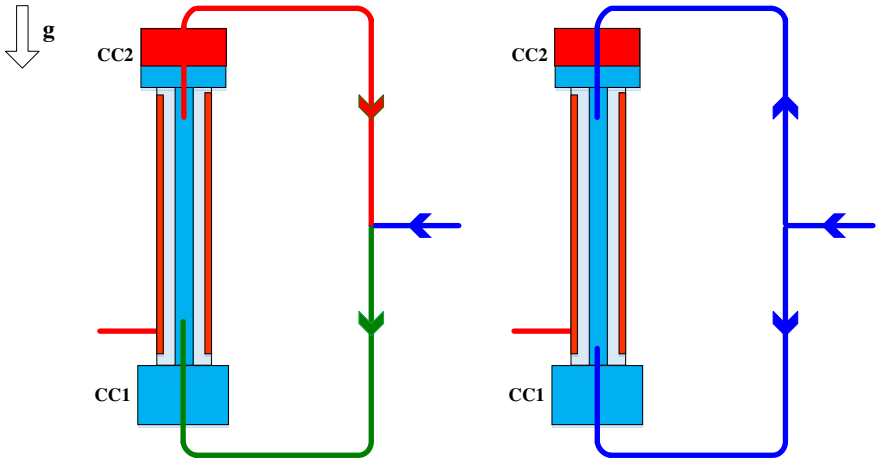


(a) local natural circulation (b) forced flow

Fig. 9 Schematic of the local natural circulation and forced flow in terrestrial surroundings

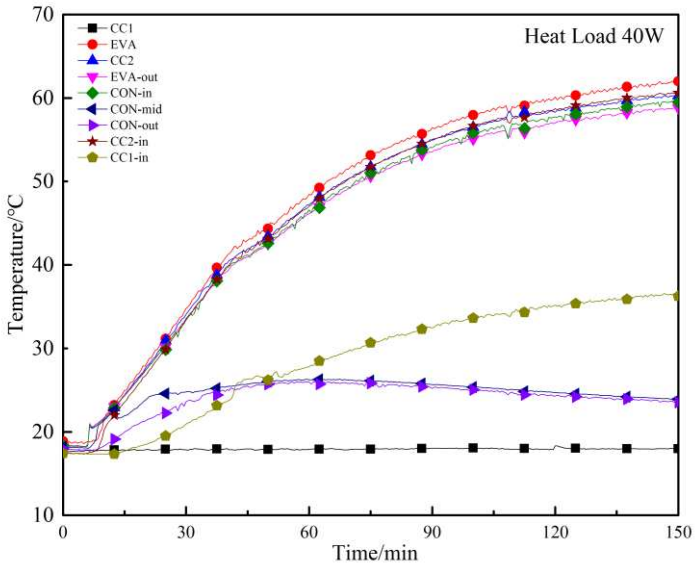


Fig. 10 Startup at a heat load of 40W at 45° tilt angle

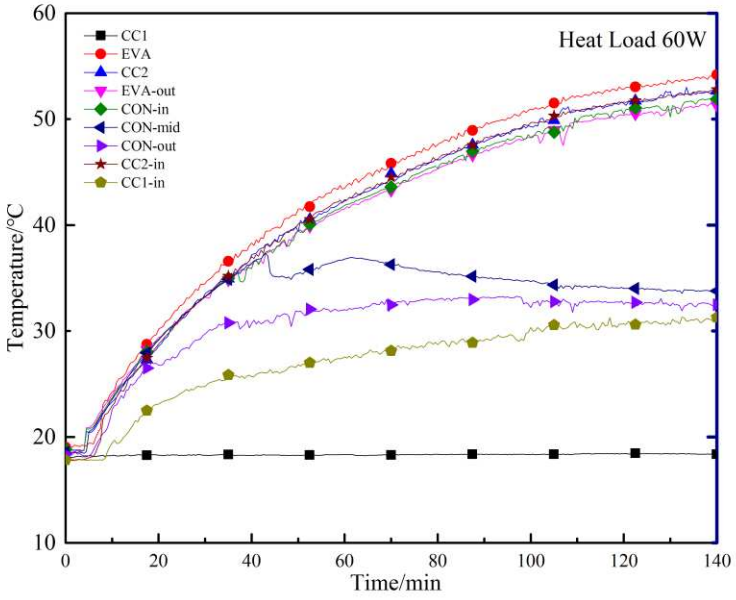


Fig. 11 Startup at a heat load of 60W at 45° tilt angle

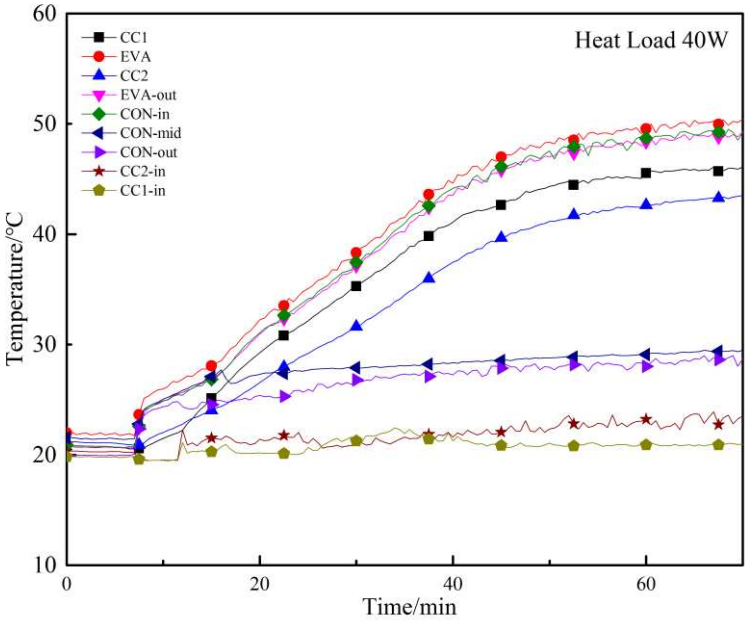


Fig. 12 Startup at a heat load of 40W in the horizontal attitude

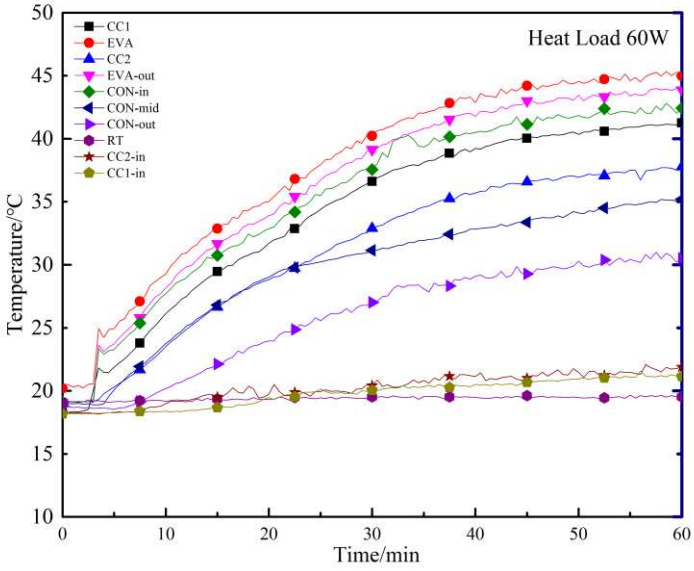


Fig. 13 Startup at a heat load of 60W in the horizontal attitude

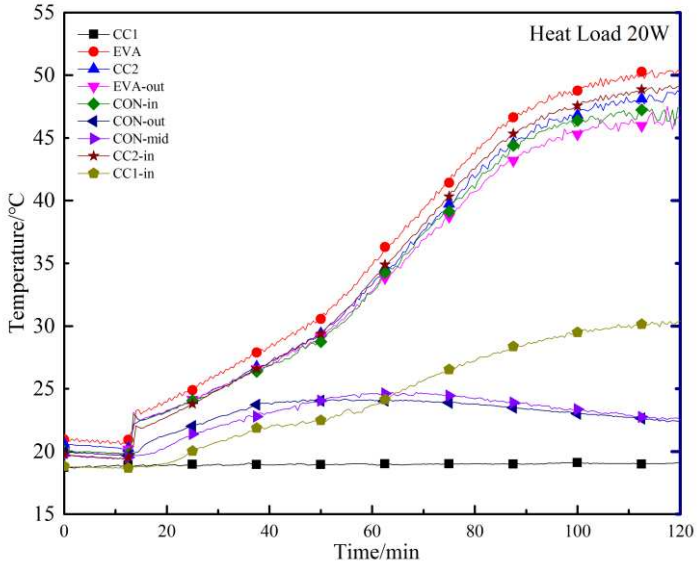


Fig. 14 Startup at a heat load of 20W in the vertical attitude

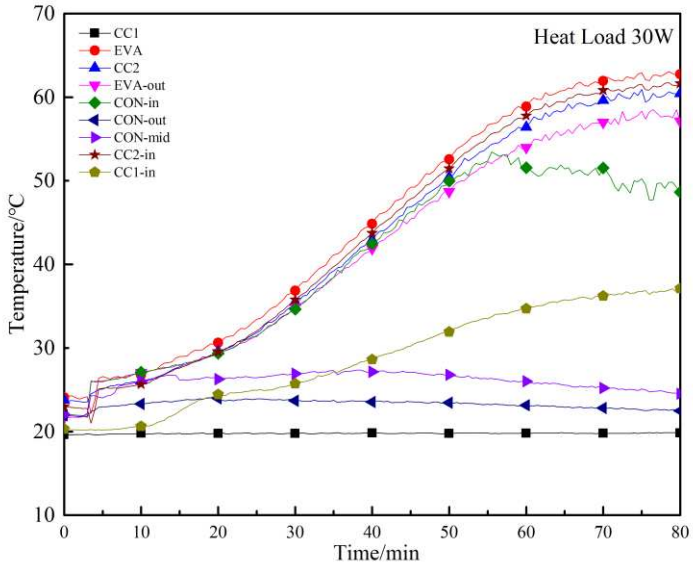


Fig. 15 Startup at a heat load of 30W in the vertical attitude

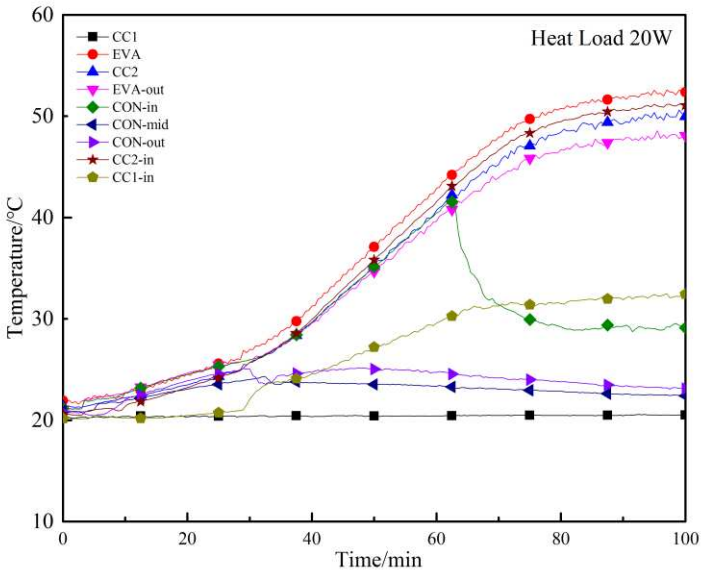


Fig. 16 Startup at a heat load of 20W in the vertical attitude with 0.3m adverse elevation

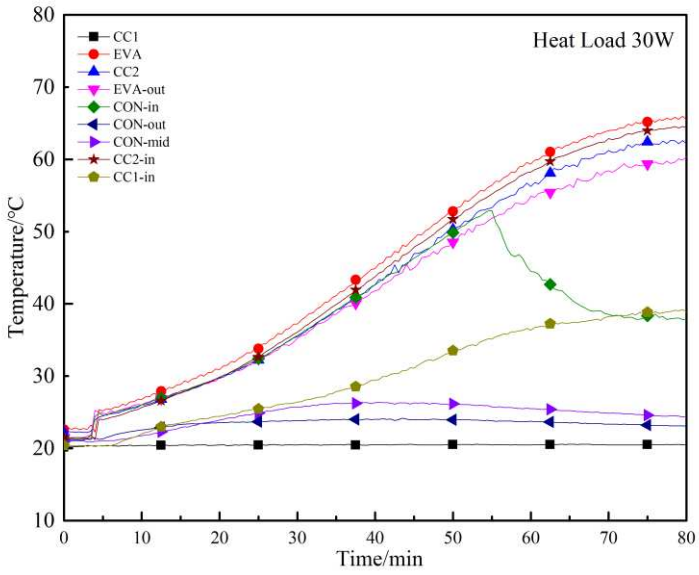


Fig. 17 Startup at a heat load of 30W in the vertical attitude with 0.3m adverse elevation

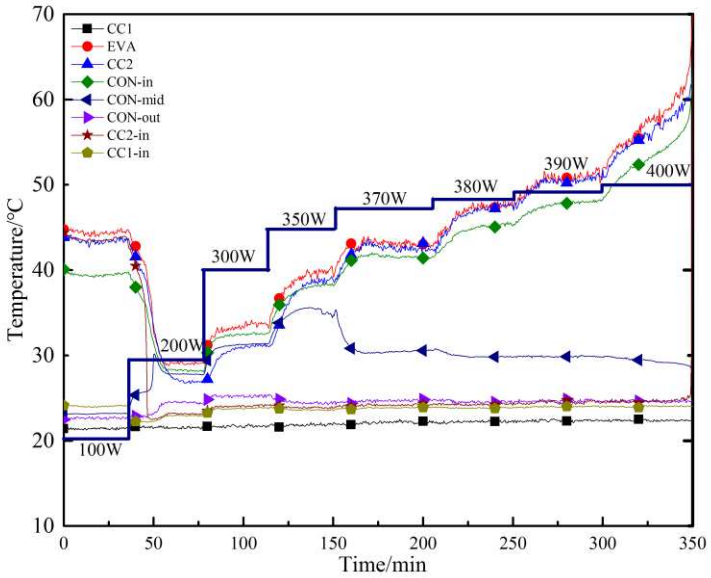


Fig. 18 Power increment test of the DCCLHP in the vertical attitude with 0.3m adverse elevation

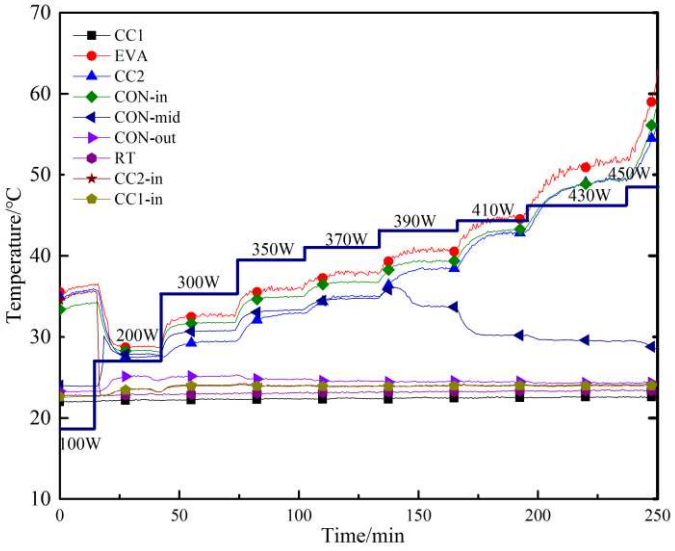


Fig. 19 Power increment test of the DCCLHP at 45° tilt angle

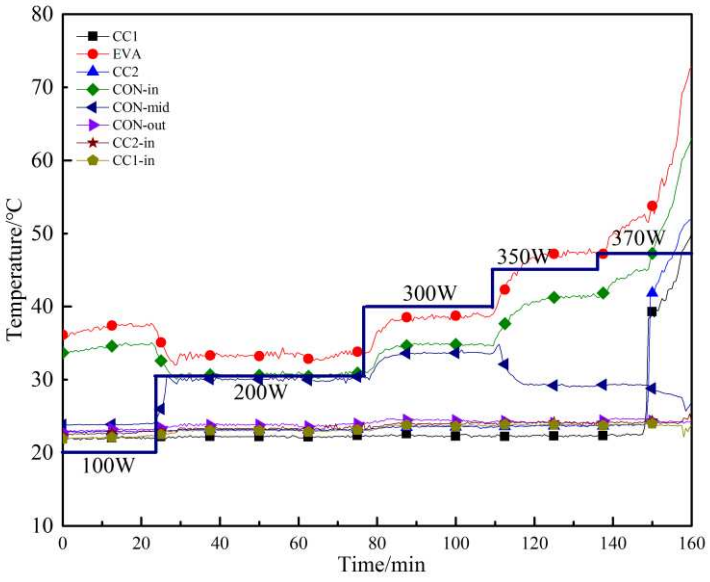


Fig. 20 Power increment test in the horizontal attitude with 0.1m adverse elevation